Refractive index determination of nanoparticles in suspension using nanoparticle tracking analysis

Edwin van der Pol[1,2], Frank A.W. Coumans[1,2], Auguste Sturk[2], Rienk Nieuwland[2], Ton G. van Leeuwen[1]*

(1) Biomedical Engineering and Physics; (2) Laboratory of Experimental Clinical Chemistry, Academic Medical Center, University of Amsterdam, Amsterdam, The Netherlands

* corresponding author

SUPPORTING INFORMATION

Transmission electron microscopy of urinary vesicles

To analyze the vesicle standard by TEM, vesicles were isolated by centrifugation (12·1000 µL, 60 minutes, 18,900 g, 4 °C). From each aliquot, 900 µL was collected for ultra-centrifugation, the next 75 µL was discarded, and the remaining 25 µL contained the relatively large vesicles. The 900 µL aliquots were ultra-centrifuged (60 minutes, 154,000 g, 4 °C) to collect smaller vesicles from the pellet. All pellets present in the remaining 25 µL from both centrifugation speeds were resuspended in 975 µL PBS citrate and centrifuged as before. For both centrifugation speeds, the washed pellets were pooled to a final volume of 300 µL. Each pool was prepared as follows: 145 µL was diluted with 145 µL PBS containing 0.2 % paraformaldehyde (w/v). After fixation for 24 hours, 10 µL was applied to a formfar-carbon coated 300 mesh grid (Electron Microscopy Sciences, Hatfield, USA) for 7 minutes, followed by staining with 1.75 % uranyl acetate (w/v). Samples were allowed to dry at room temperature for 2 hours and imaged with TEM (CM-10, Philips, Eindhoven, The Netherlands) at 100 kV.

Next, 1000 vesicles were segmented manually using the Quick selection tool of PHOTOSHOP v11.0.2 (Adobe Systems, San Jose, CA). Overlapping vesicles were included in the analysis as their boundaries could be clearly observed. A custom-made Javascript saved the surface area of the segmented vesicles to a .csv file. The vesicle size d was calculated from the surface area A using $d = \sqrt{4A/\pi}$, thereby assuming that vesicles are spherical. The overall particle size distribution (PSD) was obtained by summation of the PSDs obtained by both centrifugation speeds.

Light scattering calculations

Optical configuration NS-500

Fig. S1A shows a schematic of the optical configuration of the NS-500. A linearly polarized 45-mW diode laser emitting at 405 nm is collimated in a flow cell to illuminate vesicles. Scattered light is collected by a microscope objective with a numerical aperture (NA) of 0.4, which is placed perpendicular to the beam. NA characterizes the range of angles over which the objective collects light and is defined as $\mathrm{NA} = n_m \sin\alpha_{max}$, where n_m is the refractive index of the medium and α_{max} is the maximum propagation angle.

Mie theory

Fig. S1B shows a spherical particle with diameter d and refractive index n_p that is illuminated by a plane electromagnetic wave propagating along the z direction and polarized in the x direction:

$$\boldsymbol{E}_i = E_{0,x} e^{i(kz-\omega t)} \hat{\boldsymbol{e}}_x \tag{1.1}$$

with $E_{0,x}$ the electric field amplitude, ω the angular frequency, t the time, $\hat{\boldsymbol{e}}_x$ the orthonormal basis vector in the direction of the positive x axis, and $k = 2\pi n_m / \lambda$ the wave number, and λ is the wavelength of the incident light in vacuum. The scattering cross section, which is a hypothetical area describing the probability of light with unit incident irradiance being scattered by the particle, is given by:

$$C_{sca} = \int_0^{2\pi}\int_0^{\pi} \frac{|\boldsymbol{X}|^2}{k^2} \sin\theta d\theta d\phi \tag{1.2}$$

with θ the polar angle, ϕ the azimuthal angle, and $\boldsymbol{X}$ the vector scattering amplitude. In the NS-500, θ and ϕ are limited by the optical aperture of the microscope objective. Consequently, θ is integrated from $\theta_1 = \theta_o - \alpha_{max}$ to $\theta_2 = \theta_o + \alpha_{max}$, with θ_o the angle between the optical axis of the objective and the propagation direction of the wave $\hat{\boldsymbol{e}}_z$. For the NS-500, $\theta_o = \pi / 2$. Since the objective has a circular geometry, ϕ_1 is expressed in terms of θ as follows[1]:

$$\phi_1 = \arcsin\left(\frac{\sin\left(\frac{1}{2}\pi - \alpha_{max}\right)}{\sin\left(\frac{1}{2}\pi - \theta_0 + \theta\right)}\right) \tag{1.3}$$

and $\phi_2 = \pi - \phi_1$. The number of steps over which θ and ϕ are integrated is 50. For a spherical particle, the vector scattering amplitude $\boldsymbol{X}$ is related to the amplitude scattering matrix elements S_j as follows:

$$\boldsymbol{X} = \left(S_2 \cos\phi\right)\hat{\boldsymbol{e}}_{\|s} + \left(S_1 \sin\phi\right)\hat{\boldsymbol{e}}_{\perp s} \tag{1.4}$$

where the basis vector $\hat{\boldsymbol{e}}_{\|s}$ is parallel and $\hat{\boldsymbol{e}}_{\perp s}$ is perpendicular to the scattering plane, which is defined by the scattering direction $\hat{\boldsymbol{e}}_r$ and the propagation direction of the wave $\hat{\boldsymbol{e}}_z$. The parameters S_1 and S_2 depend on d, n_p, n_m, k, and θ, and were calculated using the Matlab routines of Mätzler[2] that are based on the Mie theory formalism of Bohren and Huffman[3]. Since $\hat{\boldsymbol{e}}_{\|s}$ and $\hat{\boldsymbol{e}}_{\perp s}$ are orthogonal, the term $\left|\boldsymbol{X}\right|^2$ can be expressed as follows

$$\left|\boldsymbol{X}\right|^2 = \left|S_2\right|^2 \cos^2\phi + \left|S_1\right|^2 \sin^2\phi \tag{1.5}$$

Camera settings

Since the scattering power of the particles in the samples differs more than 3 orders of magnitude, each sample required different camera settings. Table S1 shows the applied camera settings.

Particle tracking parameters

Each measurement comprises videos of scattering particles undergoing Brownian motion. The videos contain 8-bit images of 640 by 480 pixels, which were processed with scripts by Blair and Dufresne in Matlab (v7.13.0.564) to track the particles.[4] The script basically performs five tasks.

First, a spatial band-pass filter is applied to each image to suppress pixel noise up to 2 pixels and long-wavelength image variations down to 25 pixels. Second, a threshold of 5 is applied to each image to find local maxima to pixel level accuracy. If multiple peaks are found within a radius of 13 pixels, only the position of the brightest peak is stored. Third, each local maximum is enclosed by a window with a diameter of 25 pixels to obtain the scattering power and the centroid to sub-pixel accuracy. The scattering power is the sum of all pixel intensities within the window divided by the shutter time and camera gain response and the centroid is calculated by taking the weighted average. Particles that caused pixel saturation were omitted. Fourth, 2-dimensional trajectories are calculated from the list of particles coordinates at discrete times. The maximum allowed jump distance of a particle between two successive frames was set to 23 pixels, which corresponds to 3.9 μm. The minimum tracklength of a particle was set to 30 frames, which will be discussed in the next paragraph. From the trajectory of each particle, we calculated the mean square displacement and diffusion coefficient and related it to particle diameter via the Stokes-Einstein equation.

Minimum tracklength

The tracklength determines to what precision the diameter and scattering power are measured. A longer tracklength will increase the precision of both parameters. However, a longer tracklength also means that fewer particles are tracked, which reduces the correlation between the sample and the sampled population. Thus, the minimum tracklength determines a trade-off between precision and the number of particles included in the analysis.

To select the optimal minimum tracklength, we determined the relationship between tracklength and scattering power, diameter, and number of analyzed particles. The coefficient of variation (CV), which is the percentage ratio between the standard deviation and the mean, was used to express the reproducibility of scattering power and diameter. Fig. S2A shows the CV of the scattering power versus the minimum tracklength for 102-nm, 203-nm, and 400-nm polystyrene beads (sample 2, 3 and 4 in Table S1). To eliminate the impact of the number of analyzed particles on the CV, we determined the CV for a fixed number of beads that were at least tracked for 45 (102-nm beads) or 100 (203-nm and 400- nm beads) frames. Increasing the minimum tracklength increases the probability that a particle is in focus. Since beads are monodisperse, the mean scattering power increases and converges, whereas the standard deviation decreases. Consequently, the scattering power CV decreases with increasing minimum tracklength. Smaller beads diffuse faster than larger beads, and therefore require less tracks to converge. The average scattering power CV is 55, 47, and 43 % for tracklenghts of 15, 30, and 45 frames, respectively.

Fig. S2B shows the CV of the diameter versus the minimum tracklength for the same beads. Because the standard deviation of the determined diameter scales with $1/\sqrt{\text{tracklength}}$,

the diameter CV decreases with increasing minimum tracklength. The diameter CV is 30, 19, and 16 % for tracklenghts of 15, 30, and 45 frames, respectively.

Fig. S2C shows that the number of analyzed beads decreases with minimum tracklength. This is because particles that diffuse outside the field-of-view of the microscope before the minimum required tracklength is reached, are rejected from the analysis. Since smaller beads have a larger diffusion coefficient, smaller particles diffuse faster outside the field-of-view and are therefore more prone to rejection than larger particles. Fig. S2D shows that the number of analyzed urinary vesicles (sample 11, 12, 13 in supplemental Table S1) also decreases with tracklength. The number of events is 3843, 1280, and 567 for tracklenghts of 15, 30, and 45, respectively. A minimum tracklength of 30 frames is selected for further analysis, because the errors in diameter and illumination power are close to the best achievable (especially for vesicles < 150 nm, which is 53 % of the total), while a representative sample is still analyzed.

FIGURES

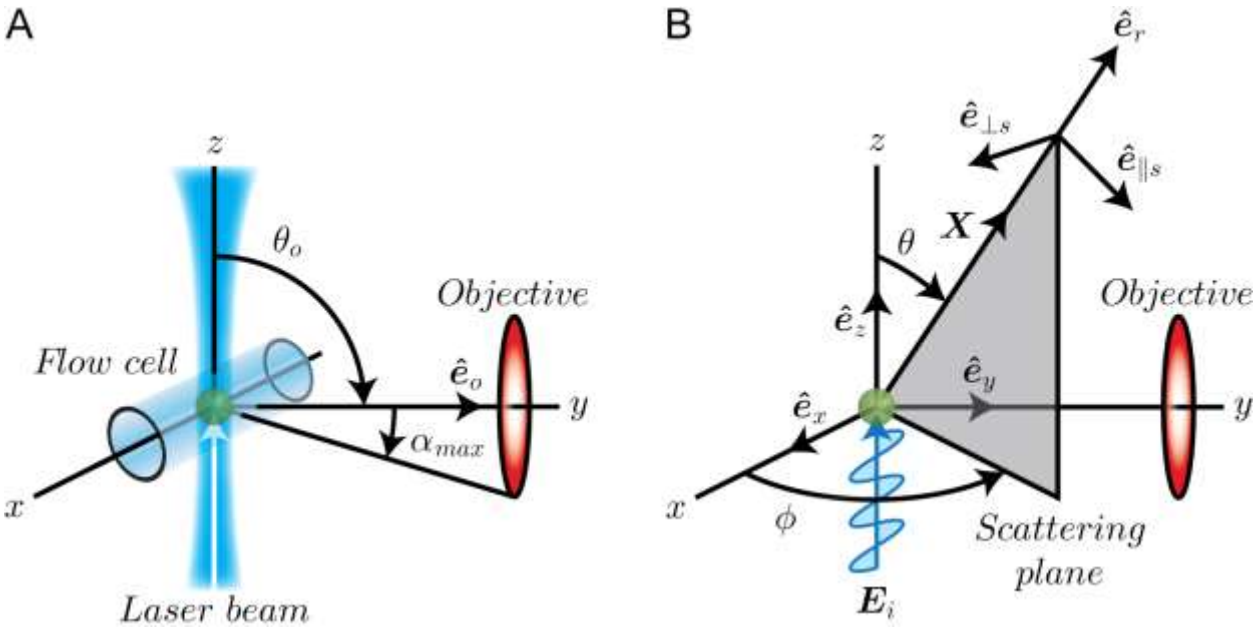

Figure S1: (A) Optical configuration of the NS-500. (B) Coordinate system and variables used to calculate the scattering intensity of a spherical particle that is illuminated by a laser beam. Symbols are explained throughout the text.

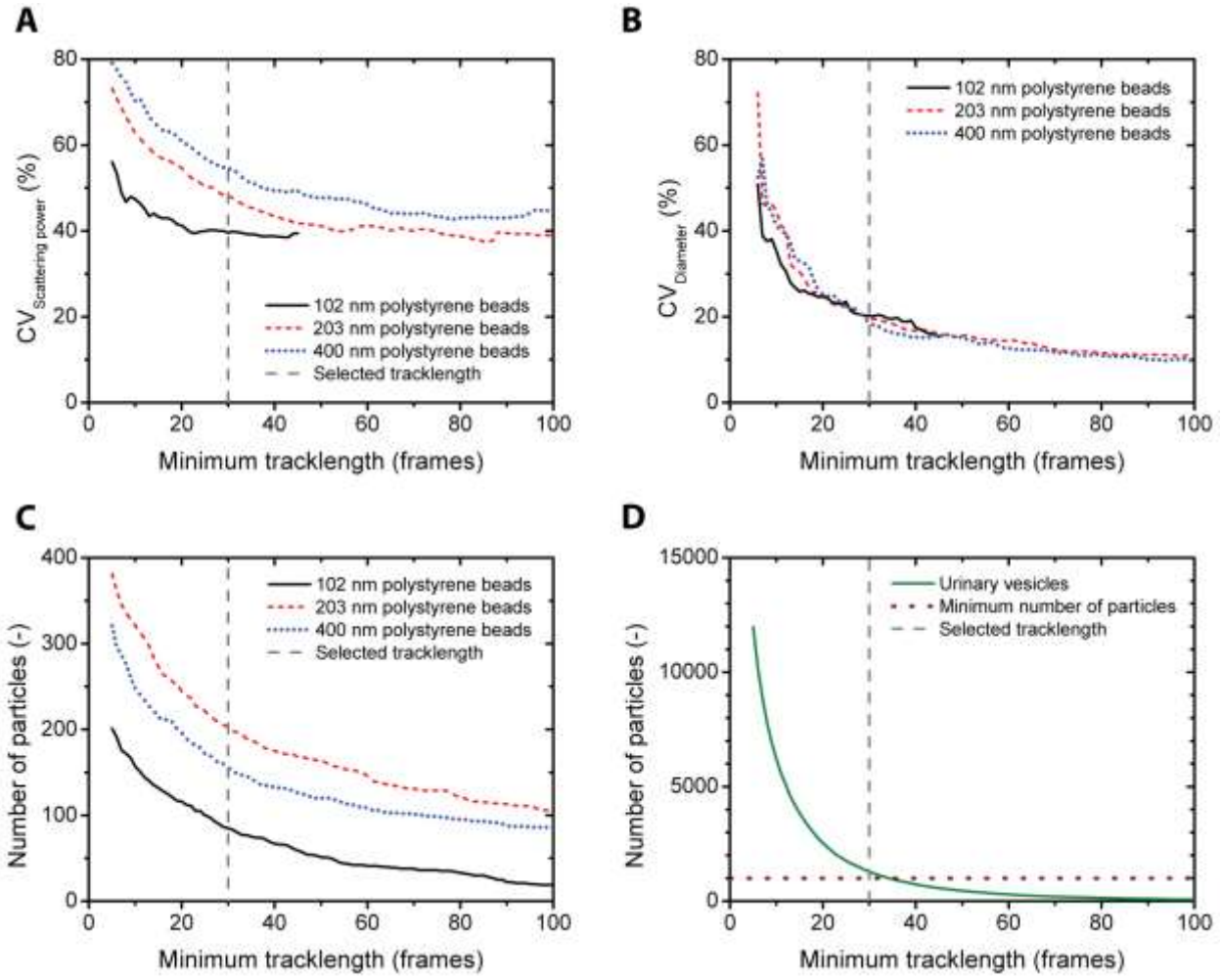

Figure S2: Impact of the minimum tracklength on the accuracy of nanoparticle tracking analysis. (A) Coefficient of variation (CV) of the scattering power, (B) CV of the diameter, (C) and number of particles versus tracklength for 102-nm (solid black line), 203-nm (dashed red line), and 400-nm (dotted blue line) polystyrene beads. CV is de defined as standard deviation divided by mean. (D) Number of particles versus tracklength for urinary vesicles. An increase of the minimum tracklength reduces the CV on scattering power and diameter, but also reduces the number of analyzed particles. To have a Poisson error ≤ 3 %, the minimum required number of analyzed particles is 1,000 (horizontal dotted line). Therefore, we selected a minimum tracklength of 30 frames (vertical dashed lines).

TABLES

Sample	d (nm)	C (mL^{-1})	Shutter time (ms)	Gain (-)	Valid tracks
1. Polystyrene beads	46	10^8	23.3	425	136
2. Polystyrene beads	102	10^8	30.0	0	134
3. Polystyrene beads	203	10^8	2.67	0	235
4. Polystyrene beads	400	10^8	0.83	0	226
5. Polystyrene beads	596	10^8	0.50	0	231
6. Silica beads	89	10^8	23.3	370	297
7. Silica beads	206	10^8	35.0	0	98
8. Silica beads	391	10^8	10.0	0	286
9. Silica beads	577	10^8	4.67	0	233
10. Beads mixture	203 & 206	$2 \cdot 10^8$	5.0	0	1744
11. Urinary vesicles	n/a	n/a	35.0	100	93
12. Urinary vesicles	n/a	n/a	35.0	350	446
13. Urinary vesicles	n/a	n/a	35.0	470	741

Table S1: Sample characteristics, applied camera settings, and number of valid tracks. *d*, diameter; *C*, concentration.

REFERENCES

(1) Fattaccioli, J.; Baudry, J.; Emerard, J. D.; Bertrand, E.; Goubault, C.; Henry, N.; Bibette, J. Size and fluorescence measurements of individual droplets by flow cytometry. *Soft Matter* **2009,** *5* (11), 2232-2238.

(2) Mätzler, C. *MATLAB functions for Mie scattering and absorption*;2002-11; Institut für Angewandte Physik, 02.

(3) Bohren, C. F.; Huffman, D. R. *Absorption and scattering of light by small particles;* Wiley: New York, NY, 1983.

(4) *The Matlab particle tracking code repository,* Georgetown University: Washington, DC, USA, 2008